Solid-State NMR Line Shapes of Uniaxially Oriented Immobile Systems

ARTICLE *in* JOURNAL OF THE AMERICAN CHEMICAL SOCIETY · AUGUST 1999

Impact Factor: 12.11 · DOI: 10.1021/ja9821910

Solid-State NMR Line Shapes of Uniaxially Oriented Immobile Systems

Alexander A. Nevzorov,[†] Stephan Moltke,[‡] Maarten P. Heyn,[§] and Michael F. Brown*

Contribution from the Department of Chemistry, University of Arizona, Tucson, Arizona 85721
Received June 23, 1998. Revised Manuscript Received May 24, 1999

Abstract: The problem of simulating the spectral line shapes of aligned immobile samples arises in solid-state NMR of various biological systems, including integral membrane proteins and peptides, receptor-bound ligands, and macroscopically oriented DNA fibers. An important issue with regard to the extraction of structural information is the correct treatment of the distribution of local symmetry axes relative to the average alignment axis (mosaic spread). Previous formulations have not considered explicitly the three-dimensional uniaxial character of the local axis disorder. Rather, the mosaic spread has been treated simply by convoluting the theoretical line shape function with an effectively two-dimensional distribution of the local symmetry axes. Here a closed-form line shape expression is derived for an axially symmetric distribution of bond orientations, which includes the uniaxial distribution of the local symmetry axis about the average alignment axis. As an illustration, the influences of the bond orientation and the degree of mosaic spread on deuterium (^{2}H) NMR line shapes are investigated. The closed-form solution in terms of elliptic integrals gives virtually identical results to those of an alternative numerical Monte Carlo line shape simulation method. The derived line shape function yields the correct powder-type limit, and has been tested by simulating a tilt series of ^{2}H NMR spectra of purple membranes containing bacteriorhodopsin with a specifically deuterated 1*R* methyl group in the retinal ring. The probability distribution for the bond orientations derived herein can be of potential interest for solid-state NMR spectroscopy of aligned biomolecules involving dipolar, quadrupolar, and chemical shift interactions, such as integral membrane proteins and peptides.

Introduction

Solid-state NMR spectroscopy provides a unique tool in structural chemistry for investigating the properties of molecular solids, liquid crystals, and various supramolecular biological assemblies.[1−9] Here, the structural parameters are contained in the principal values of the coupling tensor due to quadrupolar, dipolar, or chemical shift interactions, together with the orientation of the principal axes of the tensor relative to the external magnetic field.[10] Magic-angle spinning studies [11,12] can provide the tensor principal values in terms of internuclear distance constraints,[13] which are analogous to those in nuclear Overhauser effect spectroscopy (NOESY) in solution NMR.[14,15] Likewise, solid-state NMR of oriented samples[3,16] yields angular constraints, corresponding to the limit of weak alignment in solution NMR, e.g., involving bicelles[17] or filamentous phage.[18] For noncrystalline or amorphous systems, comparison of the solid-state NMR line shapes with theory allows one to investigate the static distributions of bond orientations, the pre-averaging due to fast motions, and the degree of static disorder in aligned samples.

In certain cases one deals with the simulation of solid-state NMR line shapes for uniaxially oriented samples that are essentially immobile on the relevant NMR time scale. The problem of a uniaxial immobile distribution arises in noncrystalline samples of biological systems having cylindrical symmetry, including aligned biopolymers such as RNA or DNA,[8,19] integral

* To whom correspondence should be addressed.

[†] Work based in part on a dissertation submitted in partial fulfillment of the requirements for the Ph.D. degree in Chemistry at the University of Arizona. Present address: Department of Chemistry and Chemical Biology, Baker Laboratory, Cornell University, Ithaca, NY 14853.

[‡] Present address: Institute of Structural Biology, Forschungszentrum Jülich, D-52425 Jülich, Germany.

[§] Also at: Department of Biochemistry, University of Arizona, Tucson, AZ 85721, and Department of Physics, Freie Universität Berlin, Arnimallee 14, D-14195 Berlin, Germany.

(1) Vold, R. R. In *Nuclear Magnetic Resonance of Liquid Crystals*; Emsley, J. W., Ed.; D. Reidel Publishing Company: Dordrecht, 1985; pp 253−288.

(2) Griffin, R. G.; Beshah, K.; Ebelhäuser, R.; Huang, T. H.; Olejniczak, E. T.; Rice, D. M.; Siminovitch, D. J.; Wittebort, R. J. In *The Time Domain in Surface and Structural Dynamics*; Long, G. J., Grandjean, F., Eds.; Kluwer Academic Publishers: Dordrecht, 1988; pp 81−105.

(3) Ketchem, R. R.; Hu, W.; Cross, T. A. *Science* **1993**, *261*, 1457−1460.

(4) Cross, T. M. *Annu. Rep. NMR Spectrosc.* **1994**, *29*, 123−167.

(5) Brown, M. F. In *Biological Membranes. A Molecular Perspective from Computation and Experiment*; Merz, K., Jr., Roux, B., Eds.; Birkhäuser: Basel, 1996; pp 175−252.

(6) Brown, M. F.; Chan, S. I. In *Encyclopedia of Nuclear Magnetic Resonance*; Grant, D. M., Harris, R. K., Eds.; Wiley: New York, 1996; Vol. 2, pp 871−885.

(7) Herzfeld, J.; Hu, J. G. In *Encyclopedia of Nuclear Magnetic Resonance*; Grant, D. M., Harris, R. K., Eds.; Wiley: New York, 1996; Vol. 2; pp 862−870.

(8) Vold, R. R. In *Encyclopedia of Nuclear Magnetic Resonance*; Grant, D. M., Harris, R. K., Eds.; Wiley: New York, 1996; Vol. 5, pp 3314−3320.

(9) Brown, M. F.; Nevzorov, A. A. *Colloids Surf.* **1999**, in press.

(10) Häberlen, U. *High Resolution NMR in Solids. Selective Averaging*; Academic Press: New York, 1976.

(11) McDowell, L. M.; Schaefer, J. *Curr. Opin. Struct. Biol.* **1996**, *6*, 624−629.

(12) Griffin, R. G. *Nat. Struct. Biol.* **1998**, *5*, 508−512.

(13) Hong, M. *J. Magn. Reson.* **1999**, *136*, 86−91.

(14) Wüthrich, K. *NMR of Proteins and Nucleic Acids*; John Wiley: New York, 1986.

(15) Cavanaugh, J.; Fairbrother, W. J.; Palmer, A. G., III.; Skelton, N. J. *Protein NMR Spectroscopy. Principles and Practice*; Academic Press: San Diego, 1996.

(16) Moltke, S.; Nevzorov, A. A.; Sakai, N.; Wallat, I.; Job, C.; Nakanishi, K.; Heyn, M. P.; Brown, M. F. *Biochemistry* **1998**, *37*, 11821−11835.

(17) Tjandra, N.; Bax, A. *Science* **1997**, *278*, 1111−1114.

(18) Hansen, M. R.; Mueller, L.; Pardi, A. *Nat. Struct. Biol.* **1998**, *5*, 1065−1074.

(19) Nevzorov, A. A.; Moltke, S.; Brown, M. F. *J. Am. Chem. Soc.* **1998**, *120*, 4798−4805.

10.1021/ja9821910 CCC: $18.00
Published on Web 08/06/1999

membrane proteins,[16,20,21] filamentous phage, and possibly low-temperature lipid phases. In such applications, one is typically interested in obtaining bond angle distributions relative to the static alignment tensor of the system. Clearly the accuracy of the solid-state NMR spectral simulations is a crucial factor with regard to the reliability of biophysical interpretations. Only if there is an accurate correspondence of the simulated NMR spectra to experiment can firm conclusions be drawn about the bond angles or the degree of static disorder in the sample. Measurements of the experimental NMR line shapes as a function of the sample inclination (tilt) and temperature provide important tests for models which describe the solid-state NMR spectra for a given system,[16] as different formulations may fit the experimental line shape at a single tilt angle or temperature equally well.

Here we present a general formulation for the solid-state NMR line shapes of uniaxially oriented immobile samples for the spin $I = 1$ case. A closed-form line shape expression is derived, and the effect of the bond orientation and static disorder on deuterium (^{2}H) NMR line shapes is investigated theoretically at different macroscopic sample inclinations. As a representative example, an integral membrane protein which plays an important role in photosynthetic energy conversion, bacteriorhodopsin, is considered.[16] The new line shape simulation method can be applied to solid-state NMR spectra involving quadrupolar, dipolar, and chemical shift interactions as a means of studying biomolecular structure in relation to activity, e.g., for integral membrane protein receptors having bound ligands.[22]

Solid-State NMR Line Shapes of Uniaxially Aligned Immobile Samples

In what follows, we consider the specific case of the quadrupolar coupling in deuterium (^{2}H) NMR spectroscopy, as in the pioneering work of Vold and co-workers.[1,8,23−25] However, the analysis is generally applicable to quadrupolar, dipolar, and chemical shift interactions as a result of the isomorphism of the Hamiltonians for rank-2 interactions.[10] To calculate the line shape function due only to static distributions, and possible pre-averaging of the coupling tensor from fast motions (on the ^{2}H NMR time scale), one needs to calculate the marginal probability distribution of the NMR transition frequencies.[5] The latter depends on all of the possible orientations of the C−^{2}H bonds in the sample. For spin $I = 1$ quadrupolar nuclei, a closed-form line shape expression can be derived by considering the single-quantum transitions $|+1\rangle \rightarrow |0\rangle$ and $|0\rangle \rightarrow |-1\rangle$, corresponding to the ^{2}H NMR transition frequencies ν_Q^+ and ν_Q^-, respectively, as given by[6]

$$\nu_Q^{\pm} = \pm \frac{3}{4}\chi \left\{ D_{00}^{(2)}(\Omega_{XL}) - \frac{\eta}{\sqrt{6}}\left[D_{-20}^{(2)}(\Omega_{XL}) + D_{20}^{(2)}(\Omega_{XL}) \right] \right\} \quad (1)$$

In the above expression, the subscript $X \equiv P, I$ designates the frame associated with the principal axis system (PAS, P) of the *static* electric field gradient (EFG) tensor, or alternatively the intermediate (I) frame of the *residual* EFG tensor (i.e., left-over from motions fast on the ^{2}H NMR scale); and L denotes the laboratory frame defined by the external main magnetic field $\mathbf{B_0}$. An example of the case of a static EFG tensor would be an immobile C^2H_2 group, whereas a rapidly rotating C^2H_3 group would yield a residual coupling tensor. A more detailed discussion of tensor averaging can be found in the book chapter of Brown.[5] In eq 1, $\chi \equiv \chi_Q$ or χ_Q^{eff} is the static or residual (effective) quadrupolar coupling constant, and $\eta \equiv \eta_Q$ or η_Q^{eff} is the asymmetry parameter of the EFG tensor. The symbols $D_{n0}^{(2)}(\Omega_{XL})$, where $n = 0, \pm 2$, denote the Wigner rotation matrix elements for the overall transformation of the irreducible components of the EFG tensor from its static or residual principal axis system, associated with a particular ^{2}H-labeled site, to the laboratory frame as given by the Euler angles $\Omega_{XL} = (\tilde{\phi}, \tilde{\theta}, 0)$. Here we use the convention of Rose[26] for right-handed body-fixed rotations, and for the Wigner rotation matrixes.

The generalized coupling parameters χ and η are related to the principal values of the EFG tensor and can be determined from the powder-type ^{2}H NMR spectrum, for which the bond directions are isotropically distributed.[10] Comparison of the residual coupling parameters χ_Q^{eff} and η_Q^{eff} to the appropriate static values χ_Q and η_Q yields information about the influences of pre-averaging due to fast motions.[5,8] For instance, in case of a methyl group, fast rotations lead to a reduction of the static coupling constant by a factor of 3, viz. $\chi_Q^{\text{eff}} = \chi_Q\ {}^1/_2\ (3\cos^2 109.47° - 1) = -{}^1/_3\ \chi_Q = -56.7$ kHz, where the effective asymmetry parameter η_Q^{eff} is reduced to zero by the axially symmetric motions.

Deuterium (^{2}H) NMR Spectroscopy of Aligned Systems. One approach for simulating solid-state NMR spectra is to derive a closed-form line shape function, which is limited to fairly simple distributions, such as spherical powder-type averaging.[5,9,27−33] A closed-form expression for the ^{2}H NMR line shapes in the case of a simple distribution of C−^{2}H or C−C^2H_3 bond orientations on a cone has also been derived, i.e., for conical (or cylindrical) averaging, without explicit treatment of the three-dimensional disorder of the symmetry axes.[5,20,34] A second approach involves numerical simulation of the solid-state NMR spectral line shapes, [2,35−39] e.g., by solving the stochastic Liouville−von Neumann equation including multiple-site jumps.[2,39−41] Such numerical methods are useful when the time

(20) Ulrich, A. S.; Watts, A. *Solid State Nucl. Magn. Reson.* **1993**, *2*, 21−36.
(21) Ulrich, A. S.; Watts, A.; Wallat, I.; Heyn, M. P. *Biochemistry* **1994**, *33*, 5370−5375.
(22) Salamon, Z.; Brown, M. F.; Tollin, G. *Trends Biochem. Sci.* **1999**, in press.
(23) Vold, R. L.; Vold, R. R. *Prog. Nucl. Magn. Reson. Spectrosc.* **1978**, *12*, 79−133.
(24) Vold, R. R.; Vold, R. L. *Adv. Magn. Opt. Reson.* **1991**, *16*, 85−171.
(25) Vold, R. R. In *Nuclear Magnetic Resonance Probes of Molecular Dynamics*; Tycko, R., Ed.; Kluwer Academic Publishers: Dordrecht, 1994; pp 27−112.
(26) Rose, M. E. *Elementary Theory of Angular Momentum*; Wiley: New York, 1957.
(27) Pake, G. E. *J. Chem. Phys.* **1948**, *16*, 327−336.
(28) Cohen, M. H.; Reif, F. *Solid State Phys.* **1957**, *5*, 321−438.
(29) Abragam, A. *The Principles of Nuclear Magnetism*; Oxford University Press: London, 1961.
(30) Seelig, J. *Q. Rev. Biophys.* **1977**, *10*, 353−418.
(31) Davis, J. H. *Biochim. Biophys. Acta* **1983**, *737*, 117−171.
(32) Spiess, H. W. In *NMR Basic Principles and Progress*; Diehl, P., Fluck, E., Kosfeld, R., Eds.; Springer-Verlag: Heidelberg, 1978; Vol. 15, pp 55−214.
(33) Schmidt-Rohr, K.; Spiess, H. W. *Multidimensional Solid State NMR and Polymers*; Academic Press: San Diego, 1994.
(34) Hentschel, R.; Silescu, H.; Spiess, H. W. *Polymer* **1981**, *22*, 1516−1521.
(35) Griffin, R. G. *Methods Enzymol.* **1981**, *72*, 109−174.
(36) Müller, K.; Meier, P.; Kothe, G. *Prog. Nucl. Magn. Reson. Spectrosc.* **1985**, *17*, 211−239.
(37) Schneider, D. J.; Freed, J. H. *Adv. Chem. Phys.* **1989**, *73*, 387−527.
(38) Wittebort, R. J.; Olejniczak, E. T.; Griffin, R. G. *J. Chem. Phys.* **1987**, *86*, 5411−5420.
(39) Greenfield, M. S.; Ronemus, A. D.; Vold, R. L.; Vold, R. R. *J. Magn. Reson.* **1987**, *72*, 89−107.
(40) Meier, P.; Ohmes, E.; Kothe, G. *J. Chem. Phys.* **1986**, *85*, 3598−3614.
(41) Alam, T. M.; Drobny, G. P. *Chem. Rev.* **1991**, *91*, 1545−1590.

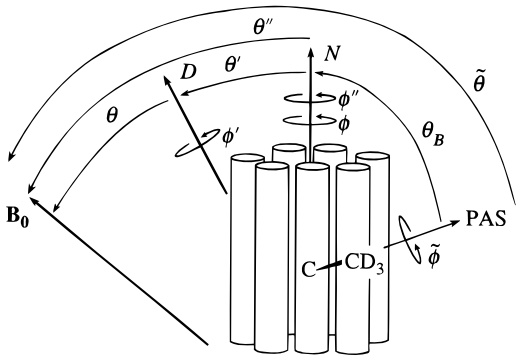

Figure 1. Example of transformation of the coupling tensor for an aligned uniaxial immobile sample. A seven-helix transmembrane protein having a ^{2}H-labeled methyl group is depicted, as in the case of bacteriorhodopsin, ref 16. The overall rotation from the principal axis system (PAS) to the laboratory frame (defined by the magnetic field $\mathbf{B_0}$) is given by the Euler angles $\Omega_{XL} \equiv (\tilde{\phi}, \tilde{\theta}, 0)$, where an axially symmetric coupling tensor ($\eta = 0$) is assumed. Using the geometry of the system, the transformation is decomposed into three intermediate rotations. The first set of Euler angles $\Omega_{XN} \equiv (0, \theta_B, \phi)$ describes the orientation θ_B of the principal axis system (PAS) of the EFG tensor, i.e., static ($X = P$) or residual ($X = I$), with respect to the local symmetry axis N, about which there is a static uniaxial distribution of the bond orientations ϕ. The second transformation $\Omega_{ND} \equiv (0, \theta', \phi')$ corresponds to the deviation θ' of the local alignment axis N with respect to the average normal to the membrane plane D (mosaic spread), together with the corresponding azimuthal rotation ϕ'. Finally, the third transformation $\Omega_{DL} \equiv (0, \theta, 0)$ describes the inclination θ (tilt) of the average membrane normal D relative to the main external magnetic field $\mathbf{B_0}$, for which the azimuth is immaterial. Note that the overall transformation from the local membrane frame to the laboratory is described by the angles $\Omega_{NL} \equiv (\phi'', \theta'', 0)$, cf. the text.

scale of the motions falls within the relevant NMR time scale, and the distribution function for the symmetry axes and the geometry of the system of interest still remain fairly simple.

Now in ^{2}H NMR spectroscopy the structural information is contained in the principal values of the electric field gradient coupling tensor, together with the orientation of its principal axes relative to the external magnetic field, as described in the classic book of Häberlen.[10] Without taking into account any specific internal molecular geometry, the overall transformation of the PAS of the static or residual EFG tensor to the laboratory frame is given in terms of the Euler angles $\Omega_{XL} = (\tilde{\phi}, \tilde{\theta}, 0)$. The latter can be expanded into three intermediate transformations, as illustrated in Figure 1 for the specific example of a seven-helix transmembrane protein having a specifically ^{2}H-labeled methyl group. Here the transformations include the orientation of the C$-^2$H or C$-$C^{2}H$_3$ bond with respect to the local symmetry axis (membrane normal), the static distribution of the local symmetry axes with respect to the average membrane normal (mosaic spread), and the orientation of the sample as a whole with respect to the external magnetic field (tilt angle). By using the well-known closure property of the rotation group,[5] one can write that

$$D^{(2)}_{n0}(\Omega_{XL}) = \sum_{m'=-2}^{2} \sum_{m=-2}^{2} D^{(2)}_{nm'}(\Omega_{XN}) D^{(2)}_{m'm}(\Omega_{ND}) D^{(2)}_{m0}(\Omega_{DL}) \quad (2)$$

Let us consider the general case of a uniaxially symmetric sample having an axially symmetric coupling tensor ($\eta = 0$). Here we start with the orientation of the principal axis system (PAS) with its z-axis along a particular C$-^2$H or C$-$C^{2}H$_3$ bond. The first set of Euler angles $\Omega_{XN} \equiv (0, \theta_B, \phi)$ pertains to the orientation of the PAS of the static or residual EFG tensor associated with the average orientation of the C$-^2$H or C$-$C^{2}H$_3$ bond with respect to the local symmetry axis (N, membrane normal), as given by the fixed angle θ_B, together with the uniaxial distribution of the bond orientations relative to the local symmetry axis ϕ. Clearly one objective of the NMR experiments is to determine θ_B accurately even in the presence of considerable mosaic spread.[16] The second transformation $\Omega_{ND} \equiv (0, \theta', \phi')$ corresponds to the local symmetry axis disorder, characterized by θ', as well as the three-dimensional uniaxial distribution of the *local* symmetry axes (N) with respect to the *average* symmetry axis (D, director) as given by the azimuthal angle ϕ'. Finally, the third transformation $\Omega_{DL} \equiv (0, \theta, 0)$ describes the fixed sample inclination (tilt) θ relative to the external magnetic field ($\mathbf{B_0}$); cf. Figure 1. (Note that the first and second transformations include the azimuth from the subsequent rotation to simplify the notation, which is consistent with the standard convention for Euler angles.[26])

However, to derive the line shape function in closed form, it is convenient to break up the transformation of eq 2 into two independent subtransformations, that is to say:

$$D^{(2)}_{00}(\Omega_{XL}) = \sum_{m=-2}^{2} D^{(2)}_{0m}(\Omega_{XN}) D^{(2)}_{m0}(\Omega_{NL}) \quad (3)$$

$$D^{(2)}_{00}(\Omega_{NL}) = \sum_{m=-2}^{2} D^{(2)}_{0m}(\Omega_{ND}) D^{(2)}_{m0}(\Omega_{DL}) \quad (4)$$

Referring to Figure 1, the additional angles Ω_{NL} (ϕ'', θ'', 0) describe the overall orientation of the local symmetry axis N with respect to the laboratory frame (main magnetic field), which can be expressed via the Euler angles θ' and ϕ'. To simplify the analytical calculation, rank-1 rotation matrixes can be used instead of rank-2, which yields

$$\cos\tilde{\theta} = \cos\theta_B \cos\theta'' - \sin\theta_B \sin\theta'' \cos(\phi + \phi'') \quad (5)$$

$$\cos\theta'' = \cos\theta' \cos\theta - \sin\theta' \sin\theta \cos\phi' \quad (6)$$

(In using rank-1 rotation matrixes it must be remembered that the parity is odd, whereas the coupling interaction has even parity and is invariant to inversion [42].) Here ϕ'' is a phase factor (not shown) that is a function of (θ', ϕ'). It links the combined closure expressions using two transformations, given above, with the full closure expansion of eq 2 using three transformations. The additional phase can be disregarded when the azimuthal average is considered,[16] or when differentiating holding (θ', ϕ') constant (vide infra). The angles ϕ and ϕ' are uniformly distributed from 0 to 2π, whereas the probability distribution of the angle θ' can be approximated in many cases simply by a normal Gaussian distribution. At a given displacement from the average director θ', the marginal probability distribution of the bond angles $\tilde{\theta}$ can then be obtained by integrating the joint probability for the multivariate distribution over (θ',ϕ') or equivalently θ'', which is the corresponding polar angle (co-latitude).

Probability Distribution for Overall Bond Orientation. Clearly one is generally interested in the distribution of the overall bond angle $\tilde{\theta}$ with respect to the laboratory frame, as defined by the magnetic field $\mathbf{B_0}$. The task at hand is then, first, to evaluate the mapping of the joint probability distribution for the angular variables (θ', ϕ') into the probability distribution for the overall bond angle $\tilde{\theta}$. Second, the mapping of the overall

(42) Trouard, T. P.; Alam, T. M.; Brown, M. F. *J. Chem. Phys.* **1994**, *101*, 5229−5261.

bond angle distribution $p(\tilde{\theta})$ into the distributions for the reduced frequencies $\xi_\pm$ of the two $I = 1$ spectral branches is considered, where the latter constitute the experimental NMR line shape.[5] In the limit of a random or spherical (powder-type) distribution, $p(\tilde{\theta}) \rightarrow {}^1/_2 \sin \tilde{\theta}$ and the well-known Pake doublet is obtained.[27,29] But for a semi-random distribution, e.g., a uniaxial or conical-type distribution, $p(\tilde{\theta})$ is governed by the specific geometry appropriate to the problem considered.[5]

In terms of the model depicted in Figure 1, the static distribution of $\tilde{\theta}$ is specifically generated by the azimuthal rotation ϕ about the local symmetry axis, e.g., the local membrane normal. That is to say, $\tilde{\theta}$ is implicitly a function of ϕ and vice versa, cf. eq 5. Thus we can write specifically that

$$p(\tilde{\theta})\,\mathrm{d}\tilde{\theta} = p[\phi(\tilde{\theta})]\,\mathrm{d}\phi(\tilde{\theta}) \equiv p(\phi)\,\mathrm{d}\phi = \frac{\mathrm{d}\phi}{2\pi} \tag{7}$$

Introducing the reduced frequencies $\xi_\pm$ of the two $I = 1$ spectral branches, the derivative $\mathrm{d}\phi/\mathrm{d}\xi_\pm$ can be evaluated to yield the NMR line shape, e.g., in the absence of mosaic spread.[5]

However, in the presence of mosaic spread (alignment disorder), the overall bond angle $\tilde{\theta}$ or alternatively ϕ depends on the two angular variables (θ', ϕ'), in addition to the fixed parameters (θ, θ_B). Here one needs to consider the marginal probability distribution for the random variable $\tilde{\theta}$ obtained by integrating over the variables (θ', ϕ'). In general, the marginal probability distribution for $\tilde{\theta}$ is obtained by integrating the joint probability density $p(\tilde{\theta}, \theta', \phi')$ with respect to the subset of variables (θ',ϕ'), yielding:

$$p(\tilde{\theta})\,\mathrm{d}\tilde{\theta} = \int_{\theta'=0}^{\pi} \int_{\phi'=0}^{2\pi} p(\tilde{\theta}, \theta', \phi') \sin\theta'\,\mathrm{d}\theta'\,\mathrm{d}\phi' \tag{8}$$

Now according to Bayes' rule,[43]

$$p(\tilde{\theta}, \theta', \phi') = p(\tilde{\theta}|\theta', \phi')\,p(\theta')\,p(\phi') \tag{9}$$

where $p(\tilde{\theta}|\theta', \phi')$ is the conditional probability distribution for $\tilde{\theta}$ given (θ',ϕ'), and the random variables (θ',ϕ') are assumed statistically independent with probability densities $p(\theta')$ and $p(\phi')$. Comparison with eq 7 then allows one to identify the conditional probability distribution for the overall bond orientation $\tilde{\theta}$ as:

$$p(\tilde{\theta}|\theta', \phi')\,\mathrm{d}\tilde{\theta} = \frac{(\partial\phi)_{\theta',\phi'}}{2\pi} \tag{10}$$

Finally, one obtains from eqs 8−10 that

$$p(\tilde{\theta})\,\mathrm{d}\tilde{\theta} = \int_0^{\pi} \int_0^{2\pi} \frac{(\partial\phi)_{\theta',\phi'}}{2\pi} \frac{(\partial\phi')_{\theta'}}{2\pi} p(\theta') \sin\theta'\,\mathrm{d}\theta' \tag{11}$$

where ϕ and ϕ' are given in terms of eqs 5 and 6, respectively.

One can then express the above integral, eq 11, in terms of the new angular variable θ'' which describes the mosaic spread at constant θ', cf. Figure 1. Making the substitution of θ'' for ϕ' leads to

$$p(\tilde{\theta})\mathrm{d}\tilde{\theta} = \frac{1}{4\pi^2} \int_0^{\pi} \int_{\theta-\theta'}^{\theta+\theta'} \left(\frac{\partial\cos\phi}{\partial\tilde{\theta}}\right)_{\theta',\theta''} \left(\frac{\partial\cos\phi'}{\partial\theta''}\right)_{\theta'} \times \frac{\mathrm{d}\tilde{\theta}}{\sin\phi} \frac{\mathrm{d}\theta''}{\sin\phi'} p(\theta') \sin\theta'\,\mathrm{d}\theta' \tag{12}$$

After calculating the derivatives in eq 12, the probability distribution $p(\tilde{\theta})$ for rank-2 interactions becomes

$$p(\tilde{\theta})\mathrm{d}\tilde{\theta} = \frac{1}{4\pi^2} \int_0^{\pi} \int_{\cos(\theta+\theta')}^{\cos(\theta-\theta')} \times \frac{\mathrm{d}\cos\theta''}{\sqrt{[\cos(\tilde{\theta} - \theta_B) - \cos\theta''][\cos\theta'' - \cos(\tilde{\theta} + \theta_B)]}} \times \frac{p(\theta')\sin\theta'\,\mathrm{d}\theta'\sin\tilde{\theta}\,\mathrm{d}\tilde{\theta}}{\sqrt{[\cos(\theta - \theta') - \cos\theta''][\cos\theta'' - \cos(\theta + \theta')]}} \tag{13}$$

Note that in the above expression $\tilde{\theta}$ and θ_B are treated as constant parameters, so that the integral involves the single integration variable θ'' within the above indicated limits. It is well-known that a unique solution for such an integral equation is not obtained.[44] Physical solutions for eq 13 are obtained only for the case that the square roots are both real. In what follows, we define

$$\alpha \equiv \cos(\tilde{\theta} - \theta_B) \tag{14a}$$

$$\beta \equiv \cos(\tilde{\theta} + \theta_B) \tag{14b}$$

$$\gamma \equiv \cos(\theta - \theta') \tag{14c}$$

$$\delta \equiv \cos(\theta + \theta') \tag{14d}$$

Physical considerations (cf. Figure 1) indicate that for angles $\tilde{\theta}$, θ_B, θ, and $\theta' \in [0, \pi]$ the inequalities $\cos(\tilde{\theta} - \theta_B) \geq \cos(\tilde{\theta} + \theta_B)$ and $\cos(\theta - \theta') \geq \cos(\theta + \theta')$ are applicable. Consideration of the various permutations of the cosine terms in the two radicands (not shown) then yields two real physical solutions: (*i*) for $\alpha > \gamma > \delta > \beta$ or $\gamma > \alpha > \beta > \delta$, and (*ii*) for $\gamma > \alpha > \delta > \beta$ or $\alpha > \gamma > \beta > \delta$.

NMR Spectral Frequencies and Line Shape Function. Following ref 5 one next needs to consider mapping of the probability distribution for the overall bond angle $\tilde{\theta}$ into the frequency space of the NMR spectrum. For an axially symmetric coupling tensor, the NMR spectrum is given in terms of the reduced frequencies $\xi_\pm$ of the two $I = 1$ spectral branches by[5]

$$\xi_\pm = \pm\,{}^1/_2\,(3\cos^2\tilde{\theta} - 1) \tag{15}$$

corresponding to $|\cos\tilde{\theta}| = \sqrt{(1\pm2\xi_\pm)/3}$. Conservation of probability in the angular or frequency spaces then yields:

$$p(\xi_\pm)\,\mathrm{d}\xi_\pm = p(\tilde{\theta})\,\mathrm{d}\tilde{\theta} \tag{16}$$

However, due to the even-rank coupling, only the absolute value can be determined, so that

$$p(\xi_\pm) \rightarrow |p(\xi_\pm)| = \left|\frac{\mathrm{d}\tilde{\theta}}{\mathrm{d}\xi_\pm}\right| |p(\tilde{\theta})| \tag{17a}$$

$$= \frac{|p(\tilde{\theta})|}{\sqrt{3(1 \pm 2\xi_\pm)}\,|\sin\tilde{\theta}|} \tag{17b}$$

We are now in a position to calculate the line shape function $p(\xi_\pm)$ in mathematical closed form. The distribution of the colatitude $p(\theta')$ is assumed to be Gaussian

$$p(\theta') = \frac{1}{\sigma\sqrt{2\pi}} \exp\left(\frac{-\theta'^2}{2\sigma^2}\right) \tag{18}$$

(43) van Kampen, N. G. *Stochastic Processes in Physics and Chemistry*; North-Holland: Amsterdam, 1981.

(44) Gradshteyn, I. S.; Ryzhik, I. M. *Table of Integrals, Series, and Products, 5th ed.*; Academic Press: San Diego, 1994.

where σ is the standard deviation about the mean of $\langle\theta'\rangle = 0$. Integration of eq 13 with respect to cos θ'' then yields two physical solutions which involve complete elliptic integrals of the first kind.[44] (A similar approach is used in the case of an asymmetric coupling tensor.[5]) The following general expression is obtained for the NMR line shape:

(i) if $\alpha > \gamma > \delta > \beta$ or $\gamma > \alpha > \beta > \delta$

$$|p(\xi_\pm)| \propto \frac{1}{|\cos\tilde{\theta}|}\int_0^\pi \frac{1}{y}\boldsymbol{K}\left(\frac{x}{y}\right)\exp\left(\frac{-\theta'^2}{2\sigma^2}\right)\sin\theta'\,d\theta' \quad (19a)$$

(ii) if $\gamma > \alpha > \delta > \beta$ or $\alpha > \gamma > \beta > \delta$

$$|p(\xi_\pm)| \propto \frac{1}{|\cos\tilde{\theta}|}\int_0^\pi \frac{1}{x}\boldsymbol{K}\left(\frac{y}{x}\right)\exp\left(\frac{-\theta'^2}{2\sigma^2}\right)\sin\theta'\,d\theta' \quad (19b)$$

where

$$x \equiv \sqrt{(\gamma-\delta)(\alpha-\beta)} \quad (19c)$$

$$y \equiv \sqrt{(\alpha-\delta)(\gamma-\beta)} \quad (19d)$$

Here the kernel $\boldsymbol{K}(k) = F(\pi/2,k)$ represents a complete elliptic integral of the first kind in the normal trigonometric form[44]

$$\boldsymbol{K}(k) = \int_0^{\pi/2}\frac{dx}{\sqrt{1-k^2\sin^2 x}} \quad (20)$$

The reader should note that the $\pm$ solutions correspond to the reduced frequencies $\xi_\pm$ so that $\cos\tilde{\theta} = +\sqrt{(1\pm2\xi_\pm)/3}$, $-\sqrt{(1\pm2\xi_\pm)/3}$.

Clearly the above general result, eqs 19a−d, for an immobile uniaxial distribution in the presence of three-dimensional alignment disorder should reduce directly in various limiting cases to previous formulations.[5,20] For instance, in the absence of mosaic spread ($\theta' = \phi' = 0$), the probability density $p(\theta')$ becomes $\delta(\theta'-0) = \delta(\cos\theta'-1)$, i.e., a Dirac delta function is obtained. Solution (i) then gives

$$|p(\xi_\pm)| \propto \frac{1}{|\cos\tilde{\theta}|}\int_0^\pi \frac{1}{y}\boldsymbol{K}\left(\frac{x}{y}\right)\delta(\cos\theta'-1)\,d\cos\theta' \quad (21a)$$

$$\propto \frac{1}{|\cos\tilde{\theta}|}\frac{1}{y}\boldsymbol{K}\left(\frac{x}{y}\right)\Big|_{\cos\theta'=1} \quad (21b)$$

and analogously for solution (ii). In this limit only solution (i) yields a physical result; whereas the contribution from solution (ii) becomes zero. Thus, eqs 19a−d reduce immediately to the previously published result for a conical semi-random distribution in the absence of mosaic spread[5,20]

$$|p(\xi_\pm)| \propto \frac{1}{|\cos\tilde{\theta}|\sqrt{[\cos(\theta+\theta_B)-\cos\tilde{\theta}][\cos\tilde{\theta}-\cos(\theta-\theta_B)]}} \quad (22)$$

Here $\cos(\tilde{\theta}-\theta_B) > \cos\theta > \cos(\tilde{\theta}+\theta_B)$, which is satisfied for all angles. The above expression, eq 22, is equivalent to the case when only eq 5 is considered,[20] for which the theoretical line shape function must be convoluted with a Gaussian distribution, replacing $\theta \rightarrow \theta \pm \theta'$ to introduce the mosaic spread. However, this approach corresponds to an effectively two-dimensional treatment of the alignment disorder, since eq 5 by itself contains no information about the *uniaxial* character of the distribution of the local symmetry axes, as manifested by *both* the angles θ' and ϕ'. (In geographical terms one includes only latitude whereas longitude is neglected.) Consequently, one needs to properly treat the uniaxial distributions about both the local membrane normal and the average membrane normal, as described by eqs 5 and 6. Finally, in the limit that the integrands in eqs 19a−d are independent of $\tilde{\theta}$ the classical Pake formula[5,27,29] is obtained

$$|p(\xi_\pm)| \propto \frac{1}{|\cos\tilde{\theta}|} \quad (23a)$$

$$\propto \frac{1}{\sqrt{1\pm2\xi_\pm}} \quad (23b)$$

Alternative Monte Carlo Line Shape Simulation Method

Here we also consider an alternative numerical method for the NMR line shape simulation, which can prove useful in the case of complicated internal molecular geometries and distribution functions for the alignment disorder.[16,19] Even if an analytical closed-form expression can be derived for the probability distribution, $p(\tilde{\theta})$, it still has to be integrated over the distribution of possible orientations of the local symmetry axes with respect to the average director, cf. eqs 19a−d. The complete elliptic integrals arising in this procedure can be calculated only numerically in most cases and converge slowly due to the presence of singularities, which affect the precision and require substantial computational time. Moreover, to obtain the final inhomogeneous line shape, eqs 19a−d have to be convoluted with the intrinsic line shape, e.g., due to homogeneous linebroadening. However, these computational difficulties are bypassed if the line shape is accumulated numerically from the very beginning, namely, by randomly generating the corresponding variables such as ϕ, ϕ', and θ' according to their distribution functions, and using eqs 1 and 2 together with eqs 5 and 6. The angles ϕ and ϕ' are uniformly distributed from 0 to 2π, whereas θ' is assumed to be normally distributed with a Gaussian standard deviation σ. In the case of three-dimensional symmetry axis disorder, random values of θ' are generated by inverting the associated cumulative distribution function $P(\theta')$,

$$P(\theta') = N\int_0^{\theta'}\exp\left(\frac{-q^2}{2\sigma^2}\right)\sin q\,dq \quad (24)$$

where N is a normalization constant, and the values of $P(\theta')$ are uniformly distributed from 0 to 1. For a given triple of the angles ϕ, ϕ', and θ' the quadrupolar splitting is calculated by using eqs 1 and 2, and a unit intensity value is assigned to this splitting. This procedure, referred to as the Monte Carlo line shape simulation method, is repeated about 50 000 times which proves sufficient to accumulate a smooth spectrum from −100 to 100 kHz. Finally, the convolution with the intrinsic line shape can be numerically calculated.

Simulation of Deuterium NMR Spectra of Uniaxial Immobile Samples

Clearly any model which aims at describing the ^{2}H NMR spectra of aligned samples should reproduce a classical Pake powder pattern[27−29] as a limiting case if the angles θ' are uniformly distributed over a unit sphere, regardless of the macroscopic tilt angle of the sample. Part a of Figure 2 shows simulations of powder-type ^{2}H NMR spectra obtained by using

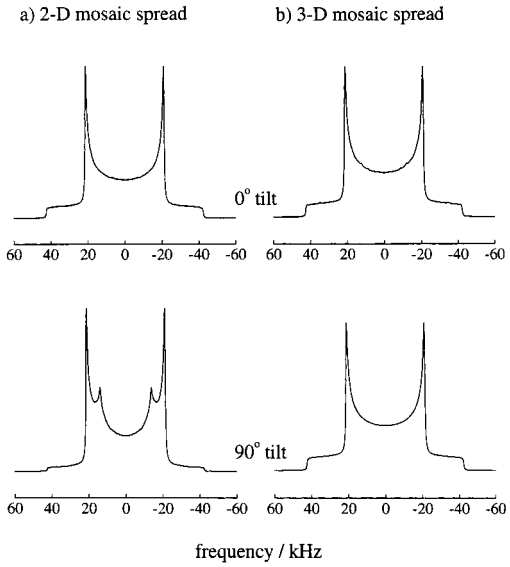

Figure 2. Simulation of ^{2}H NMR powder-type limit for a uniaxially oriented immobile sample at macroscopic inclination angles of $\theta = 0°$ and 90° using values for the effective coupling parameters of $\chi_Q^{eff} = 56.7$ kHz and $\eta_Q^{eff} = 0$, and a mosaic spread of $\sigma = 7°$. Convolution with an intrinsic Lorentzian line shape having a width of 0.5 kHz has been applied as a final step. (a) Simulation using the simplified two-dimensional distribution of symmetry axes, eq 22, obtained by replacing $\theta \rightarrow \theta \pm \theta'$ and averaging over θ'. (b) Simulation using a three-dimensional distribution of the symmetry axes, eqs 19a−d, cf. the text. Note that the formulation based on the two-dimensional distribution, part a, fails to reproduce the powder spectrum limit at 90° sample tilt. On the other hand, part b shows that the classical Pake powder pattern can be recovered as a limiting case at both tilt angles by explicitly including both the uniaxial distributions about the *N* and *D* axes, viz. involving ϕ and ϕ', corresponding to a three-dimensional treatment of the mosaic spread.

a simplified treatment for the mosaic spread, eq 22, where $\theta \rightarrow \theta \pm \theta'$, which corresponds to effectively a two-dimensional distribution of the symmetry axes. As can be seen from Figure 2, while the powder-type Pake pattern can be reproduced as a limiting case for the $\theta = 0°$ tilt angle, it cannot be simulated for the $\theta = 90°$ tilt. By contrast, use of eqs 19a−d, which correspond to a full three-dimensional treatment of the mosaic spread, eliminates this undesirable feature. Consequently a powder pattern is recovered at both tilt angles, part b, as well as at other sample inclinations θ (not shown). *The above emphasizes the importance of a correct treatment for the distribution of the symmetry axes in uniaxially aligned samples*.

Next, Figure 3 shows simulation of a tilt series of ^{2}H NMR spectra for a uniaxially oriented immobilized sample at various values of the bond orientation θ_B with respect to the local symmetry axis, as indicated in parts a−f. The closed-form line shape expression given by eqs 19a−d has been used. As can be seen, changing the value for the bond angle yields dramatic alterations of the ^{2}H NMR spectral line shapes, such as the appearance and disappearance of peaks and shoulders in the spectra, especially for tilt angles θ of 15, 30, and 45°. Note that the largest changes are predicted within the range of bond angles θ_B from 30 to 50°. By contrast, Figure 4 shows that the effect of the local axis disorder σ (mosaic spread) primarily changes the spectral line widths for different values of σ, cf. parts a−f. At a greater degree of the mosaic spread, the ^{2}H NMR spectra become similar to the powder-type Pake pattern at larger sample inclinations, cf. parts e and f of Figure 4.

A comparison of the results for a tilt series of ^{2}H NMR spectra calculated by using the closed-form line shape expression, eqs

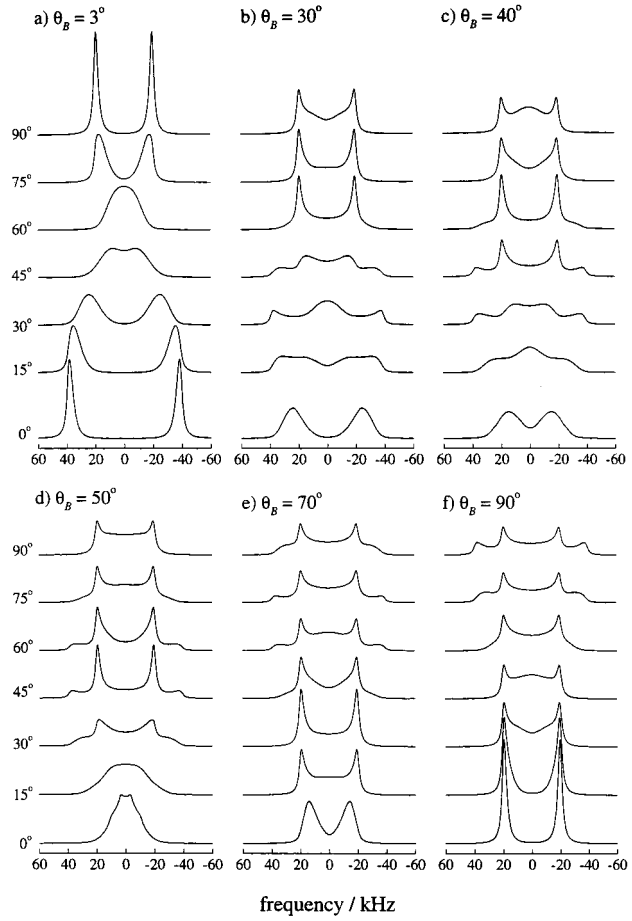

Figure 3. Simulation of tilt series of ^{2}H NMR spectra for a uniaxial immobile sample showing the effect of the bond orientation θ_B with respect to the local symmetry axis at sample inclinations of $\theta = 0°$, 15°, 30°, 45°, 60°, 75°, and 90°. All spectra are scaled by the integral: (a) $\theta_B = 3°$, (b) $\theta_B = 30°$, (c) $\theta_B = 40°$, (d) $\theta_B = 50°$, (e) $\theta_B = 70°$, and (f) $\theta_B = 90°$. The closed-form expression, eqs 19a−d, has been used together with values of the coupling constant of $\chi_Q^{eff} = 56.7$ kHz and a mosaic spread of $\sigma = 7°$. Convolution with an intrinsic Lorentzian line shape having a width of 3.2 kHz has been applied as a final step. Varying the bond orientation θ_B yields dramatic alterations of the spectral line shapes, especially for tilt angles θ of 15°, 30°, and 45° within the range of bond angles θ_B from 30 to 50°.

19a−d, with those obtained by using the Monte Carlo method is presented in Figure 5. The two methods yield virtually identical results, although the calculation time in the former case is about 60 times longer than for the Monte Carlo simulation (1 h versus less than one minute for the whole tilt series calculated on a desktop computer operating at 266 MHz). It follows that the Monte Carlo approach appears to be more effective from a computational point of view, especially for the case of a nonaxially symmetric EFG tensor and complicated internal geometries as in the case of DNA.[19] However, in terms of structural biophysics it is clearly desirable to employ both approaches as a means of investigating the uniqueness of the bond angle solutions.

Application to Integral Membrane Proteins

As a representative biological application, the closed-form line shape expression, eqs 19a−d, has been used to simulate experimental ^{2}H NMR spectra of an integral membrane protein, bacteriorhodopsin (bR), aligned on planar glass substrates.[16] Bacteriorhodopsin is a light-driven proton pump[45−47] and occurs naturally in the purple membranes of *Halobacterium salinarium*.

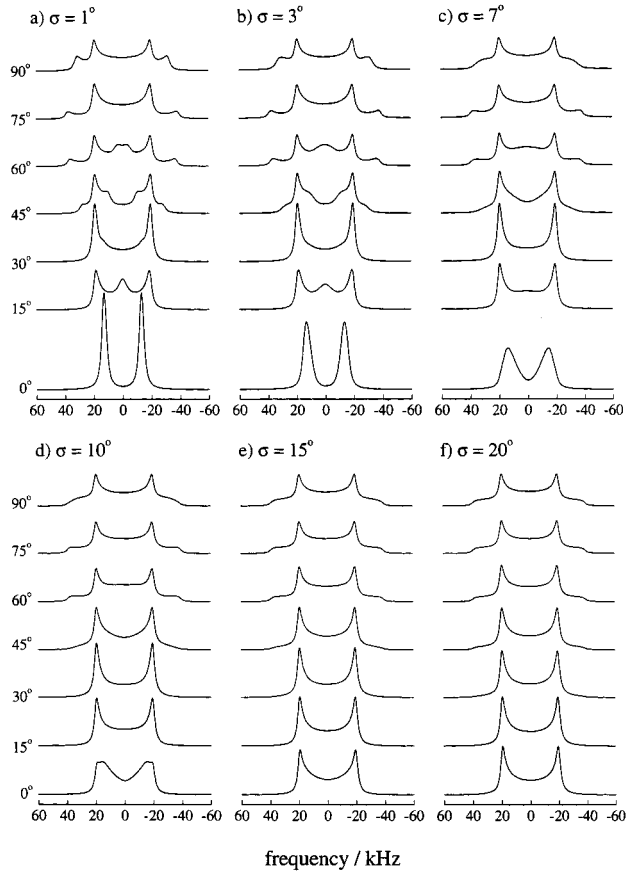

Figure 4. Simulation of tilt series of ^{2}H NMR spectra for a uniaxial immobile sample showing influence of the mosaic spread σ at sample inclinations of $\theta = 0°$, 15°, 30°, 45°, 60°, 75°, and 90°. All spectra are scaled by area: (a) $\sigma = 1°$, (b) $\sigma = 3°$, (c) $\sigma = 7°$, (d) $\sigma = 10°$, (e) $\sigma = 15°$, and (f) $\sigma = 20°$. The closed-form expression, eqs 19a−d, has been used together with values of the effective coupling constant of $\chi_Q^{eff} = 56.7$ kHz and the bond orientation of $\theta_B = 70°$. A Lorentzian line broadening of 3.2 kHz has been applied as a final step. Increasing the local axis disorder σ (mosaic spread) primarily broadens the spectral line widths. At even greater degrees of mosaic spread, the ^{2}H NMR spectra become similar to a powder-type Pake pattern at larger sample inclinations, $\theta = 60-90°$, cf. parts e and f.

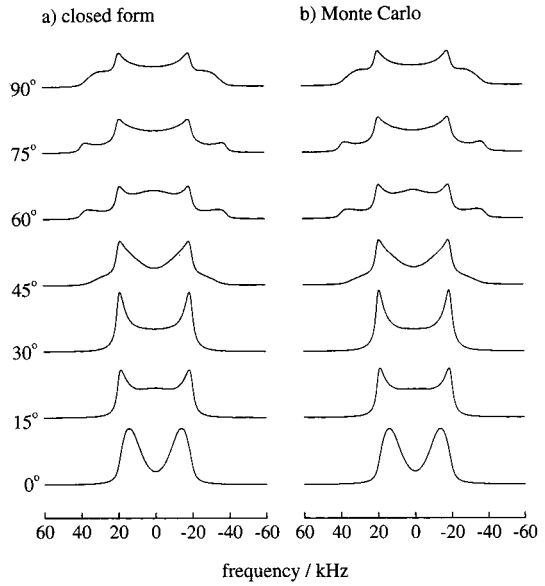

Figure 5. Comparison of results obtained using different line shape treatments: (a) closed-form line shape expression given by eqs 19a−d; (b) Monte Carlo line shape simulation using eqs 1 and 2 together with eqs 5 and 6. Results are shown for sample inclinations of $\theta = 0°$, 15°, 30°, 45°, 60°, 75°, and 90°, where all spectra are scaled by the integral. The value of the effective coupling constant has been set to $\chi_Q^{eff} = 56.7$ kHz, and the bond orientation and the mosaic spread have been fixed at values of $\theta_B = 70°$ and $\sigma = 7°$, respectively. Convolution with an intrinsic Lorentzian line shape having a width of 3.2 kHz has been applied as a final step. Note that the two methods yield virtually identical results; however, the computational time in the former case is about 60 times longer than for the Monte Carlo simulation. Therefore, the Monte Carlo approach is computationally more effective, especially for the case of a nonaxially symmetric EFG tensor and more complicated internal geometries.

It is the prototype of seven-helix transmembrane proteins and bears a similarity to other members of this class, such as rhodopsin which is found in the rod cells in animal and human eyes and plays an important role in the process of vision.[48,49] Bacteriorhodopsin thus represents a model system which can be investigated in relation to other integral membrane proteins and ligand-binding receptors.[22,50] It is known that the chromophore isomerizes about one of its double bonds after absorption of light, and in this way changes its interactions with the protein binding pocket. Hence, the structural information from ^{2}H NMR spectroscopy may be of great value in understanding the mechanisms of action of these retinal proteins.

Simulation of the experimental ^{2}H NMR tilt series spectra for macroscopically oriented purple membranes, containing bacteriorhodopsin with a specifically ^{2}H-labeled methyl group at the 1*R* position of the retinal ring,[16] is depicted in Figure 6. Fast motions about the methyl rotor axis yield a decrease of the static coupling constant[5] by approximately a factor of 3, as found from simulating the powder-type ^{2}H NMR spectrum[16] to obtain the principal values of the coupling tensor of $\chi_Q^{eff} = 52.4$ kHz and $\eta_Q^{eff} = 0$. Part a shows representative experimental ^{2}H NMR spectra of bR-containing purple membranes aligned on planar substrates.[16] As can be seen from part b of Figure 6, a three-dimensional treatment of the mosaic spread, given by eqs 19a−d, yields an excellent agreement of the simulated and experimental spectra if the bond angle θ_B is set to 68.8°. It is noteworthy that at 0° sample inclination, for a given value of the bond angle θ_B there is an additional solution ($\theta_B = 42°$, not shown in Figure 6) which yields a similar spectral pattern, but with a reversed sign of the quadrupolar splitting.[16] Therefore, to unequivocally determine the value of the bond orientation θ_B, additional spectral measurements at other sample inclinations are needed.

The necessity to consider properly the three-dimensional uniaxial character of the mosaic spread is further illustrated in part c of Figure 6. Here the simplified two-dimensional treatment of the mosaic spread[20] has been used, eq 22. The subspectra calculated for various values of $\theta \rightarrow \theta \pm \theta'$ distributed around the average macroscopic tilt angle θ have been added with a weighting factor of $\exp[-(\theta - \theta')^2/2\sigma^2]$. In this case a slightly different value for the bond orientation of $\theta_B = 69.5°$ is needed to correspond to the experimentally observed splitting at 0° tilt, in comparison with the three-dimensional treatment having $\theta_B = 68.8°$. As can be seen, the peaks corresponding to the ^{2}H

(45) Otto, H.; Marti, T.; Holz, M.; Mogi, T.; Lindau, M.; Khorana, H. G.; Heyn, M. P. *Proc. Natl. Acad. Sci. U.S.A.* **1989**, *86*, 9228−9232.
(46) Mathies, R. A.; Lin, S. W.; Ames, J. B.; Pollard, W. T. *Annu. Rev. Biophys. Biophys. Chem.* **1991**, *20*, 491−518.
(47) Alexiev, U.; Marti, T.; Heyn, M. P.; Khorana, H. G.; Scherrer, P. *Biochemistry* **1994**, *33*, 13693−13699.
(48) Brown, M. F. *Chem. Phys. Lipids* **1994**, *73*, 159−180.
(49) Brown, M. F. *Curr. Top. Membr.* **1997**, *44*, 285−356.
(50) Hruby, V. J.; Pettitt, B. M. In *Computer-Aided Drug Design. Methods and Applications*; Perun, T. J., Propst, C. L., Eds.; Marcel Dekker: Basel, 1989; pp 405−460.

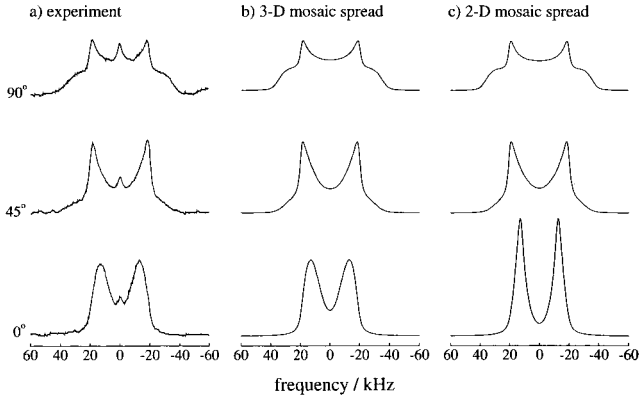

Figure 6. Simulation of experimental ^{2}H NMR spectra of bacteriorhodopsin in oriented purple membranes at different sample tilt angles at 20 °C, ref 16, showing influence of different treatments of the mosaic spread. (a) Experimental spectra at $\theta = 0°$, 45°, and 90° sample inclinations. (b) Simulation by using eqs 19a−d, corresponding to an explicit treatment of the three-dimensional uniaxial distribution of the symmetry axes, with a bond orientation of $\theta_B = 68.8°$ and a Gaussian standard deviation for the mosaic spread of $\sigma = 7.2°$. (c) Simulation using the simplified treatment, eq 22, corresponding to an effectively two-dimensional approximation for the mosaic spread, ref 20, with a bond orientation of $\theta_B = 69.5°$ and a Gaussian standard deviation of $\sigma = 7.0°$. In both cases a coupling constant of $\chi_Q^{eff} = 52.4$ kHz has been used, ref 16, and a Lorentzian linebroadening of 3.2 kHz has been applied together with a correction, ref 54, for the finite pulse length of 3.2 μs. The minor peak in the center of the experimental ^{2}H NMR spectra, part a, most likely arises from the natural abundance of deuterium in water. Excellent agreement of the theoretical spectra with experiment is obtained in the case of part b for an explicit three-dimensional treatment of the mosaic spread. By contrast, the two-dimensional formulation, part c, yields much sharper peaks at 0° sample tilt than observed experimentally, and thus is not applicable for description of the static disorder in purple membranes.

NMR splitting at $\theta = 0°$ tilt are found to be much sharper than observed experimentally, and cannot be fitted simultaneously with the rest of the tilt series. The above means that the simplified treatment, eq 22, is not suitable for the description of solid-state ^{2}H NMR spectra of uniaxially oriented integral membrane proteins. It is also interesting that if the subspectra are added together with an additional factor $\sin \theta' \, d\theta'$, the quality of the simulation for the 0° tilt ^{2}H NMR spectrum is improved (not shown). However, the reader is warned that inclusion of the sine factor to account for the three-dimensional character of the symmetry axis disorder is inconsistent with the neglect of integrating over the azimuthal angle ϕ' in the effectively two-dimensional treatment.

Discussion

Solid-state NMR spectroscopy provides a powerful tool for studying molecular solids and liquid crystals[1,6,9,24,25] as well as biological macromolecules and supramolecular assemblies. Representative biological applications include both integral membrane proteins and lipid molecules,[5,51] as well as fibrous proteins, filamentous bacteriophages, carbohydrates, and nucleic acids.[8,19,41] In the case of uniaxially aligned samples having an effectively static distribution, orientational information including bond orientations and the degree of molecular ordering (mosaic spread) can be obtained by analyzing the ^{2}H NMR line shapes, which can help to better understand the structural properties of biological solids and liquid crystalline assemblies.[5] The main factors that influence the accuracy of the various bond angles are the choice of a model for description of the geometry of the system of interest, and the type of distribution of the local symmetry axes (mosaic spread). In the present paper, a general closed-form expression has been derived for the NMR line shapes of immobile uniaxially oriented systems as a function of the macroscopic sample tilt angle. The line shape function derived in closed form has been shown to yield identical results with an alternative numerical Monte Carlo method.[16,19] However, for the case of complicated internal geometries and types of static disorder, as well as for a nonaxially symmetric electric field gradient tensor, the latter approach is advantageous, since it allows one to avoid a substantial increase in computational time associated with singularities in the closed-form line shape function.

The ^{2}H NMR line shape theory described in the present work for aligned samples can be applied to integral membrane proteins and peptides at temperatures where they are essentially immobilized to form an axially symmetric distribution about the membrane normal. Representative examples include bacteriorhodopsin[16] and possibly rhodopsin, the opioid receptors, and various G protein-coupled receptors.[22] Moreover, as shown by Nevzorov et al.[19] the same method can also be applied in principle to nucleic acid fibers and their interactions with proteins. As a specific illustration, the previously published[16] experimental tilt series of the ^{2}H NMR spectra of macroscopically oriented purple membranes, containing bacteriorhodopsin with a specifically ^{2}H-labeled methyl group at the 1*R* position of the retinal ring, has been simulated in closed form. The results show that a simplified treatment,[20] which corresponds effectively to a two-dimensional mosaic spread, does not describe simultaneously the ^{2}H NMR spectra at all tilt angles, nor can a powder pattern be recovered as a limiting case. By contrast, an excellent agreement of the simulated spectra with experiment is obtained in the case of a three-dimensional treatment. Here, the data allow one to determine the angle between the 1*R*-[1-C^{2}H$_3$] methyl group rotor axis of the retinal prosthetic group and the membrane normal to be 68.8° ± 1.0° (or alternatively its supplementary value of 180° − 68.8° = 111.2°; see Moltke et al.[16] for a more detailed discussion of experimental errors). It should be noted that such precision still lies beyond the reach of one of the most powerful methods for structure determination, namely X-ray crystallography.[52,53] The information about the various bond orientations obtained from ^{2}H NMR can then be further used as angular constraints in conjunction with other experimental techniques as a means of determining the overall orientation of the retinal with respect to the membrane normal. As a rule, the ^{2}H NMR line shape method described here can be applied to studies of ligands bound to integral membrane proteins, membrane-bound peptides, and other uniaxial aligned systems in relation to their biological mechanisms of action.

Acknowledgment. This work was supported by the U.S. National Institutes of Health (EY 12049 to M.F.B. and GM 53484 to M.P.H.) and by a postdoctoral fellowship from the Deutsche Forschungsgemeinschaft (S.M.). We also gratefully acknowledge the late Regitze R. Vold for her pioneering contributions and for sharing her insight through many stimulating comments and discussions.

JA9821910

(51) Smith, S. O.; Griffin, R. G. *Annu. Rev. Phys. Chem.* **1988**, *39*, 511−535.

(52) Pebay-Peyroula, E.; Rummel, G.; Rosenbusch, J. P.; Landau, E. M. *Science* **1997**, *277*, 1676−1681.

(53) Luecke, H.; Richter, H.-T.; Lanyi, J. K. *Science* **1998**, *280*, 1934−1937.

(54) Bloom, M.; Davis, J. H.; Valic, M. I. *Can. J. Phys.* **1980**, *58*, 1510−1517.